Steel and Composite Structures, Vol. 8, No. 1 (2008) 53-83 53
DOI: http://dx.doi.org/10.12989/scs.2008.8.1.053

Seismic design of irregular space steel frames using advanced methods of analysis

A. A. Vasilopoulos[1], N. Bazeos[1] and D. E. Beskos[1,2,*]

[1]*Department of Civil Engineering, University of Patras, GR-26500 Patras, Greece*

[2]*Office of Theoretical and Applied Mechanics, Academy of Athens, 4 Soranou Efessiou Str., GR-11527 Athens, Greece*

Abstract. A rational and efficient seismic design methodology for irregular space steel frames using advanced methods of analysis in the framework of Eurocodes 8 and 3 is presented. This design methodology employs an advanced static or dynamic finite element method of analysis that takes into account geometrical and material non-linearities and member and frame imperfections. The inelastic static analysis (pushover) is employed with multimodal load along the height of the building combining the first few modes. The inelastic dynamic method in the time domain is employed with accelerograms taken from real earthquakes scaled so as to be compatible with the elastic design spectrum of Eurocode 8. The design procedure starts with assumed member sections, continues with the checking of the damage and ultimate limit states requirements, the serviceability requirements and ends with the adjustment of member sizes. Thus it can sufficiently capture the limit states of displacements, rotations, strength, stability and damage of the structure and its individual members so that separate member capacity checks through the interaction equations of Eurocode 3 or the usage of the conservative and crude q-factor suggested in Eurocode 8 are not required. Two numerical examples dealing with the seismic design of irregular space steel moment resisting frames are presented to illustrate the proposed method and demonstrate its advantages. The first considers a seven storey geometrically regular frame with in-plan eccentricities, while the second a six storey frame with a setback.

Keywords: seismic design; irregular space steel frames; finite element method; advanced analysis methods; inelastic dynamic analysis; pushover analysis; Eurocode 8; Eurocode 3

1. Introduction

It has been recently shown by Vasilopoulos and Beskos (2006, 2008) that seismic design of regular, moment resisting, plane and space steel frames using advanced methods of analysis represents a more general, rational and efficient methodology than the conventional code-based one. This design methodology employs an advanced time domain finite element analysis that takes into account material and geometric nonlinearities and member and frame imperfections in a performance-based design framework.

In the above works (Vasilopoulos and Beskos 2006, 2008) the steel frames have been assumed to be regular both with respect to in-plan and elevation and only accidental eccentricities have been taken into account for the case of space frames. In the present work, this seismic design methodology (Vasilopoulos

*Corresponding author, E-mail: d.e.beskos@upatras.gr

and Beskos 2006, 2008) is extended to the case of irregular steel space frames, both with respect to in-plan and elevation. A simpler version of this methodology employing a static nonlinear finite element analysis (pushover analysis) instead of the dynamic one is also used for the seismic design of these irregular frames.

Seismic steel design using advanced methods of analysis can sufficiently capture the limit states of displacements, rotations, strength, stability and damage of the structure and its members directly, so that separate member capacity checks through the interaction equations of Eurocode 3 (EC 3 1992) or the use of the crude behavior factor of Eurocode 8 (EC 8 2004) are not required (Vasilopoulos and Beskos 2006, 2008). Advanced methods of analysis for plane or space regular frame design have been used in connection with steel frames under static loads (Chen and Kim 1997), reinforced concrete frames under seismic loads (Kappos and Manafpour 2001, Kappos and Panagopoulos 2004) and steel frames under seismic loads employed statically or dynamically (Mazzolani and Piluso 1996, Gioncu and Mazzolani 2002, Vasilopoulos and Beskos 2006, 2008).

Use of advanced analysis for seismic design is intimately related with the concept of performance-based design (Ghobarah 2001). The present work, being an extension of Vasilopoulos and Beskos (2006, 2008) from regular to irregular space steel frames, also combines advanced analysis with performance-based design concepts. Thus, three limit states (damage, ultimate and serviceability) are considered here and for each one of them the satisfaction or not of performance objectives dealing with storey drifts, plastic rotations, damage at the member, storey and structure level as well as plastic hinge formation pattern is checked.

According to Mazzolani and Piluso (1996) non-uniform distribution of mass, stiffness and strength in-plan of every floor or in-elevation of a framed building implies corresponding structural irregularities. The most usual types of structural irregularities in space frames are those associated with eccentricities in-plan of every floor (the mass center does not coincide with the stiffness center) and setbacks along the height of the structure. A comprehensive literature review on both of these structural irregularities up to 1993 can be found in Mazzolani and Piluso (1996). Even regular framed buildings from the geometry viewpoint, may be structurally irregular, if at every floor there exist eccentricities real or accidental. Codes always provide for accidental eccentricities even for structurally regular buildings (Vasilopoulos and Beskos 2008, EC 8 2004).

The presence of eccentricities in-plan modifies the motion of a space framed building whose floors not only translate laterally but also rotate about a vertical axis in a coupled fashion during the horizontal seismic excitation. These torsional effects produce an uneven distribution of the lateral displacements at the same level (with larger displacements at some points of the perimeter of the building) and a modification of the internal actions. Another cause of torsional effects besides eccentricities may be the asynchronous motion of the foundation of the building due to specific characteristics of the earthquake excitation, but this is not usually taken into account, except in special cases.

Most of the published work on seismic inelastic torsion of buildings due to in-plan irregularities till today is based on simplified, one storey models with simple shear-beam elements for lateral load resistance (De La Liera and Chopra 1995, Chandler *et al.* 1996, Tso and Smith 1999, Stathopoulos and Anagnostopoulos 2003, Perus and Fajfar 2005). Recent comparisons of the seismic response of single storey models, on which current codes are based, against that of multistorey models have shown the limitations of the former (Stathopoulos and Anagnostopoulos 2005). During the last three years or so, one can see studies on seismic inelastic torsional effects based exclusively on multistorey building models analysed by nonlinear dynamic finite element methods (Stathopoulos and Anagnostopoulos 2005, Marusic and Fajfar 2005) or nonlinear static (pushover) finite element methods (Kilar and Fajfar 2001, Chopra and Goel 2004).

The vertical irregularity in building frames is mainly due to the presence of setbacks. However, it can also be in geometrically regular frames due to changes in mass, stiffness and/or strength from storey to storey as a result of differences in column and/or beam sections or presence or absence of braces. The effect of vertical irregularities on the seismic response of frames has been studied (mainly) by dynamic nonlinear analyses (Humar and Wright 1977, Al-Ali and Krawinkler 1998, Chintanapakdee and Chopra 2004, Tremblay and Poncet 2005, Kappos 2005) and static nonlinear (pushover) analyses (Chintanapakdee and Chopra 2004, Kappos 2005). Most of these references deal with plane frames, which do not experience torsional motion and only very few deal with space frames with setbacks, which experience torsional motion in additional to translational one along the two horizontal directions.

Current seismic codes, such as EC 8 (2004), UBC (1997) or FEMA-273 (1997), provide some practical guidelines in order for the designer to determine if his structure is regular or not. If it is irregular, then it has to be analysed by dynamic spectral analysis. However, as it has been demonstrated by many of the aforementioned references on structural irregularities, neither the guidelines nor the suggested method of analysis are always satisfactory. Chambers and Kelly (2004) have concluded in their work that nonlinear dynamic analysis is the only option for irregular structures and urge the profession to stop resisting and start embracing what technology enables us to do. Indeed, with nonlinear dynamic analysis, torsional effects and coupling problems between translational and torsional modes are automatically taken into account. Their statement is in full agreement with the philosophy of the present work, which suggests the use of advanced methods of analysis in the seismic design of irregular framed structures. In this work, the nonlinear dynamic analysis is shown to be a rational and efficient seismic design tool. Along with this and for reasons of simplicity, the nonlinear static (pushover) analysis is also used here and successfully employed in seismic design.

2. Advanced seismic analysis fundamentals

A seismic design procedure for irregular space steel frames based on both dynamic and static advanced methods of analysis and developed in a format appropriate for incorporating into it EC 3 (1992) and EC 8 (2004) design codes in a performance-based design context is briefly presented in this section.

The advanced methods of analysis employed here take into account material and geometric non-linearities and can be divided into two basic categories: the "exact" dynamic version and the approximate simpler static (pushover) version of analysis. Both methods constitute modifications of the well known computer program DRAIN-3DX (Prakash *et al.* 1994). The seismic loads, either in their dynamic or static form, are applied on the space frames following the well known design combinations $x + 0.3z$ and $z + 0.3x$, where x and z define the two horizontal axes of the frame with the y axis being the vertical one. These lateral loads are applied at the various concentrated masses of the frame in accordance with the finite element procedure. Floor masses are concentrated at the mass center of every floor due to the assumption of diaphragm action there. Thus, torsional effects due to floor eccentricities or vertical setbacks are taken automatically into account.

Seismic loads are computed on the basis of actual design spectrum compatible accelerograms (Karabalis *et al.* 1994). Three such seismic motions are used for the design procedure and two additional ones for its verification. Static lateral loads for the pushover analysis are computed on the basis of the improved multimodal load distribution (Pavlidis *et al.* 2003).

In DRAIN-3DX (Prakash *et al.*1994) all structural members are modeled using the beam-column finite element E15 with two special plastic hinges at its ends employing the fiber model there. Thus, strain hardening, axial force-bending moment interaction and the gradual section stiffness degradation due to the axial force-bending moments interaction are taken into account. The residual stress effect is approximately taken into account by introducing into the program the tangent modulus concept. Only class 1 sections (EC 3 1992) are employed here in order to be consistent with the use of inelastic analysis and avoid local buckling. Member modeling can also consider lateral torsional buckling in an approximate manner in conformity with EC 3 (1992) by following the idea of Kim and Lee (2002). This capability has also been introduced into the program. More details can be found in Vasilopoulos and Beskos (2008).

Geometric nonlinearities including P-δ and P-Δ effects as well as imperfection effects are also taken into account. The first two nonlinearities are taken into account approximately by DRAIN-3DX (Prakash *et al.*1994). The third nonlinearity is also taken approximately into account by simply reducing the tangent modulus through its multiplication by 0.85 (Chen and Kim 1997).

Prediction of seismic damage can be easily done with the aid of various damage indices (Powell and Allahabadi 1988). The damage indices used in this work refer to the fiber, member, storey and structure level, are symbolized by I_{df}, I_{dm}, I_{ds} and I_{dg}, respectively and computed as described in Vasilopoulos and Beskos (2008). These indices have been implemented into DRAIN-3DX (Prakash *et al.*1994).

3. Advanced analysis in design

The previously described advanced analysis fundamentals are implemented here in design in conjunction with the EC 3 (1992) and EC 8 (2004) provisions and performance-based design concepts.

The matrix equation of equilibrium for a beam-column with its two potential elastic-plastic hinges at its ends connects the load vector $\{F\}$ of nodal bending moments and axial and shear forces with the deformation vector $\{d\}$ of nodal displacements and rotations as

$$\{F\} = ([K_f] \pm N|K_g|)\{d\} \tag{1}$$

where $[K_f]$ is the flexural stiffness matrix, $[K_g]$ the geometric stiffness matrix and N the axial load with + for tension and – for compression. Matrix $[K_g]$ is a function of only the length L, while $[K_f]$ a function of the moments of inertia I_y and I_z, length L, tangent modulus E_t, shear modulus G, torsional modulus J and two scalar parameters n at the two ends of the element allowing for gradual inelastic stiffness reduction there.

The tangent modulus E_t is used to account for gradual yielding effects due to residual stresses along the length of members under axial loads between two plastic hinges and has the form (Chen and Kim 1997)

$$E_t = 1.0E \text{ for } N_{sd} \le 0.5N_y$$

$$E_t = 4\frac{N_{sd}}{N_y}E\left(1 - \frac{N}{N_y}\right) \quad \text{for } N_{sd} > 0.5N_y \tag{2}$$

where $N_y = Af_y$ is the axial load at yield and E the elastic modulus. A further reduction of the elastic modulus by multiplying E_t by 0.85 is made to account for imperfections in a very simple, yet satisfactory manner (Chen and Kim 1997).

The two scalar parameters n at the two ends of the element are computed in accordance with the formula (Chen and Kim 1997)

$$n = 1 \text{ for } \alpha \leq 5$$
$$n = 4\alpha(1 - \alpha) \text{ for } \alpha > 0.5 \tag{3}$$

where α is the force-state parameter allowing for the gradual inelastic stiffness reduction at the two element ends (potential plastic hinge positions) due to possible large design shear forces and/or non-negligible lateral torsional buckling effects. Thus, with the aid of EC 3 (1992), one can express α in the form

$$\alpha = \frac{N_{sd}}{N_{pl.Rd}} + \frac{M_{ysd}}{M_{ply.Rd}} + \frac{M_{zsd}}{M_{plz.Rd}} \leq 1.0 \tag{4}$$

In the above, N_{sd} is the design axial force, $M_{y,sd}$ and $M_{z,sd}$ are the design bending moments with respect to the y (strong) and z (weak) axes of the member section, respectively, $N_{pl.Rd} = Af_y/\gamma_{M_0}$ is the axial resistance with A, f_y and $\gamma_{M_0} = 1.1$ being the cross-sectional area, the yield strength of the steel and the safety factor, respectively, and $M_{ply.Rd}$ and $M_{plz.Rd}$ denote the plastic moment resistances with respect to the y and z axes, respectively.

The moment resistances $M_{PlyRd} = W_{Ply}f_y / \gamma_{M1}$ and $M_{PlzRd} = W_{Plz}f_y / \gamma_{M1}$, where W_{Ply} and W_{Plz} are the plastic section moduli with respect to the y and z axes, respectively and $\gamma_{M1} = 1.1$ the safety factor, are appropriately reduced when design shear forces are greater than 50% of the shear force resistance (EC3 1992). The moment resistance $M_{Ply.Rd}$ is also appropriately reduced when the lateral torsional buckling effect due to possible inadequate lateral bracing of the members has to be taken into account. In that case, the above moment resistance in Eq. (4) is replaced by the reduced moment resistance M_{byRd}, which is evaluated according to EC 3 (1992) by

$$M_{byRd} = \chi_{LT} W_{ply} f_y / \gamma_{M1} \tag{5}$$

where χ_{LT} is the reduction factor for lateral torsional buckling given in EC 3 (1992) in terms of the corresponding dimensionless slenderness $\bar{\lambda}_{LT} = \lambda_{LT} / \pi(E / f_y)^{0.5}$. The slenderness λ_{LT} for lateral torsional buckling is also given in EC 3 (1992) in terms of the geometrical and material properties of the member (Vasilopoulos and Beskos 2008, EC 3 1992). It should be mentioned here that, according to EC 3 (1992), when $\bar{\lambda}_{LT} \leq 0.4$, the lateral torsional buckling effect can be neglected and Eq. (4) can be used only when the shear force exceeds 50% of the shear force resistance. If both the high shear force is

Table 1 Allowable response limits for DLS

1.	Relative storey drifts should be ≤ 1.5% of storey height h
2.	Damage indices D at member, storey and global level should be ≤ 20%
3.	Plastic rotations θ_{pl} at member ends should be ≤ $6\theta_y$, where θ_y is the rotation at first yielding, which equals $W_{pl}f_yL_b/6EI_b$ and $W_{pl}f_yL_c(1\text{-}N/N_y)/6EI_c$ for beams (b) and columns (c), respectively
4.	Plastic hinge formation only in beams (capacity design)

Table 2 Allowable response limits for ULS

1.	Relative storey drifts should be ≤ 3.0% of storey height h
2.	Damage indices D at member, storey and global level should be ≤ 50%
3.	Plastic rotations θ_{pl} at member ends should be ≤ $8\theta_y$ (θ_y defined in Table 1)
4.	Plastic hinge formation in beams and columns without collapse

small and the lateral torsional buckling effect is negligible, Eqs. (3) and (4) are omitted.

In accordance with performance-based seismic design philosophy, the proposed design procedure establishes checks on the satisfaction or not of certain design objectives at every structural performance level or limit state. The limit states considered are the serviceability limit state (SLS), the damage limit state (DLS) or life safety (LS) and the ultimate limit state (ULS) or collapse prevention (CP). The spectrum compatible seismic motions used in this work are compatible with the EC 8 (2004) elastic design spectrum defined for the DLS, ULS and SLS as described in Vasilopoulos and Beskos (2006, 2008). Tables 1 and 2 (Vasilopoulos and Beskos 2008) provide the allowable response limits for the DLS and ULS, respectively when a dynamic nonlinear analysis is employed. Only drift limits are associated with the SLS and these are equal to 0.5%*h*, where *h* is the storey height. When a static inelastic (pushover) analysis is employed, in addition to the design criteria of Tables 1 and 2, the strength ratio V_{el} / V_p of base shear forces is also considered with the indices *el* and *p* denoting elastic (dynamic spectral) and inelastic (static) analysis, respectively. This strength ratio should be 3 or 4 for DLS and 7 or 8 for ULS.

In this work, only sections of class 1 of EC 3 (1992) are used because inelastic analyses are performed and only these sections are capable of developing the full plastic moment capacity and sustaining large hinge rotations before the onset of local buckling.

4. Seismic design procedure

In the following, the sequence of the basic steps of the seismic design procedure for the two alternative ways are briefly presented.

4.1 Use of dynamic nonlinear analysis

For this case, the seismic design procedure consists of the following steps:
Step 1: Types of loads and design load combinations according to EC 3 (1992).
Step 2: Seismic load selection for the SLS, DLS and ULS.
Step 3: Preliminary member sizing on the basis of experience or simplified analyses.
Step 4: Time history analysis execution using three accelerograms for the DLS.
Step 5: Satisfaction of the DLS performance design criteria of Table 1.
Step 6: Adjustment of member sizes for the DLS.
Step 7: Verification by using two additional accelerograms for the DLS.
Step 8: Time history analysis execution using three accelerograms for the ULS.
Step 9: Satisfaction of the ULS performance criteria of Table 2.
Step 10: Seismic response using three SLS seismic records and checking of the SLS criteria.
For more details on this procedure one can consult (Vasilopoulos and Beskos 2008).

4.2 Use of static nonlinear (pushover) analysis

For this case, the seismic design procedure consists of the following steps:
Step 1: Types of loads and design load combinations according to EC 3 (1992).
Step 2: Static lateral load selection for the SLS, DLS and ULS.
Step 3: Preliminary member sizing on the basis of experience or simplified analyses.
Step 4: Dynamic spectral analysis with $q = 1$ to determine the maximum elastic base shear V_{el} for the

DLS.

Step 5: Pushover analysis at the DLS and response determination including the inelastic base shear V_p for the DLS.

Step 6: Satisfaction of the DLS performance design criteria of Table 1 and checking of the ratio V_{el}/V_p to see if it is 3 or 4 for the DLS.

Step 7: Adjustment of member sizes for the DLS.

Step 8: Pushover analysis at the ULS and response determination including the inelastic base shear V_p for the ULS

Step 9: Satisfaction of the performance design criteria of Table 2 and checking of the ratio V_{el}/V_p to see if it is 7 or 8 for the ULS.

Step 10: Seismic response by pushover analysis for the SLS and checking of the SLS design criteria.

Some explanations concerning the above pushover analysis and its design implementation are as follows:

a) According to the multimodal pushover analysis used here, the lateral forces F_d along the height of the building can be expressed as a combination of the first few modes as (Pavlidis *et al.* 2003)

$$F_d = \sqrt{(M_{1,d}^* S_{1,d})^2 + (M_{2,d}^* S_{2,d})^2 + \cdots + (M_{n,d}^* S_{n,d})^2} \tag{6}$$

with

$$S_{i,d} = [\overline{M}]\{\phi_{i,d}\}, \qquad i = 1, 2, \cdots n \tag{7}$$

In the above, the weight M_i^* is the effective mass for the i_{th} mode, $[\overline{M}]$ the generalized mass, $\{\phi_i\}$ the i_{th} mode vector, n the number of modes considered and d the x or z direction at every floor level. The diaphragm torsional moment at the mass center of every floor level is calculated as the sum of the moments $F_x e_x$ and $F_z e_z$, where e_x and e_z are the eccentricity (accidental or real) components along the x and z directions, respectively. For systems with closely spaced natural frequencies, the SRSS modal combination rule used in Eq. (6) is replaced by the CQC rule.

b) The response of the building is obtained as a result of the two possible load combinations $F_x + 0.3\ F_z$ and $F_z + 0.3\ F_x$, which for reasons of simplicity are symbolized as $x + 0.3z$ and $z + 0.3x$, respectively. This load combination is one of those mentioned in EC8 (2004). The intensity of the lateral loads is gradually increased until the drift design criterion is reached first for every limit state. At that point the remaining design criteria of the limit state considered are checked to see if they are satisfied or not.

5. Applications of the methods

The proposed seismic design methods based on dynamic and static (pushover) nonlinear analysis are applied here to two irregular space steel frames: a seven storey in-plan irregular frame and a six storey frame with a setback.

5.1 Seven storey in-plan irregular space steel frame

Consider the in-plan irregular seven storey space steel frame of Fig. 1, which also shows the numbering of the members of the frame, The x and z horizontal directions correspond to the weak and strong building axes, respectively. The first-storey height equals 3.60 m, while the next six upper storey heights are equal to 3.20 m. The bay openings along the x and z axes are equal to 5.00 m and 4.00 m,

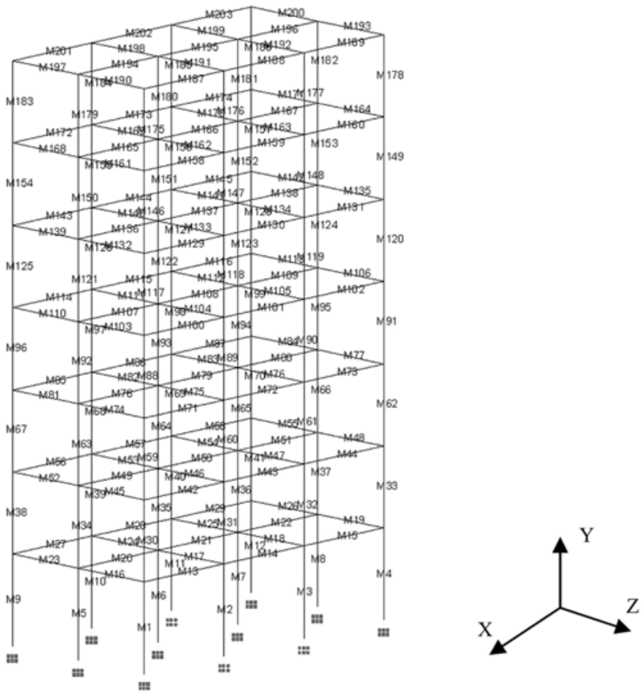

Fig. 1 Geometry and member numbering of the seven storey space steel frame

respectively. The beam and column sections of the building are IPE and HEB with S275 and S355 grade steel, respectively. The modulus of elasticity E and the shear modulus G are equal to 205 GPa and 85.4 GPa, respectively, while the strain hardening equals 3.00%. The damping is assumed to be $\xi = 0.05\%$ for the first two modes and the foundation soil of class B.

The weight density γ_s of structural steel members is 78.50 kN/m^3, while the concrete slab, the interior and exterior walls and secondary beams self weight Gs is 9.00 kN/m^2. The live loads Q are 2.00 kN/m^2. According to EC 8 (2004), the effective seismic mass corresponds to $G + 0.3Q$, where G includes the total dead weight and is placed at the mass center of each floor characterized by diaphragm type of behavior. Thus, there are only two horizontal (along the x and z axes) and one torsional component of motion (with respect to y axis) at every floor.

The seismic actions are assumed to be horizontal and are applied onto the space frame in accordance with the design combinations $x + 0.3z$ and $z + 0.3x$. Here, in spite of the apparent exterior regularity of the building, in-plan irregularities at each floor are assumed to exist. These are due to the fact that the mass center at each floor is displaced from its geometrical (stiffness) center by $\pm 0.15\, L_i$, in each horizontal direction, where L_i is the floor dimension perpendicular to the direction of the seismic action. The present building with only accidental eccentricities $\pm 0.05\, L_i$ has been designed with the aid of nonlinear dynamic analyses (Vasilopoulos and Beskos 2008). Here the eccentricities are three times larger in order to see their effect on the analysis and design results. The starting point of the design procedure using both nonlinear dynamic and static (pushover) analyses is the solution found in Vasilopoulos and Beskos (2008). This is frame F with HEB320, HEB300 and HEB280 columns for the first three, intermediate two and upper two storeys, respectively, IPE400, IPE360 and IPE330 weak axis beams for the first three, intermediate two and upper two storeys, respectively and IPE200 and IPE140 strong axis

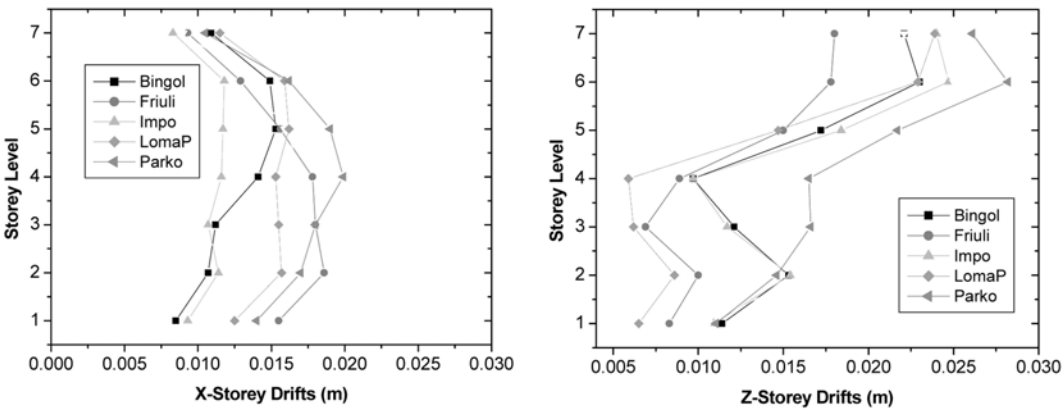

Fig. 2 Seismic drifts of frame F for all five seismic records (x + 0.3z / DLS)

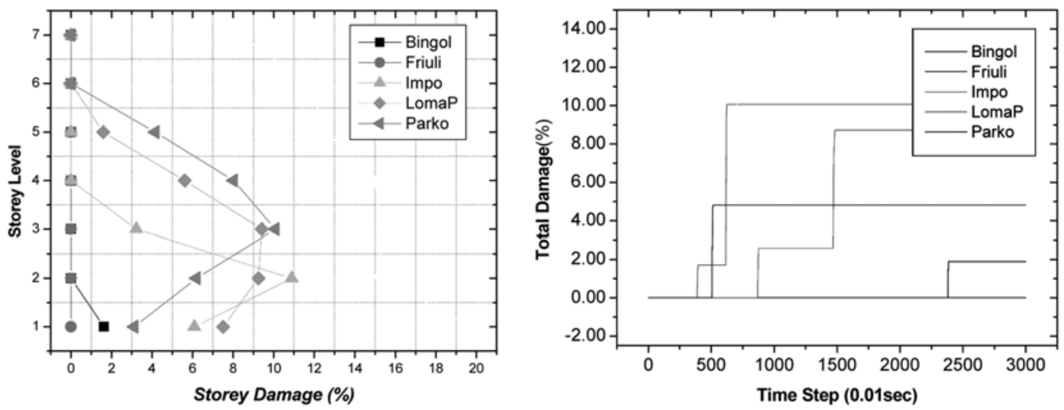

Storey Damage **Total Damage**

Fig. 3 Storey and total damage indices of frame F for all five seismic records (x + 0.3z / DLS)

beams for the first four and upper three storeys, respectively.

Results from the design procedure based on nonlinear dynamic analyses are presented first. These analyses are performed by using the DLS elastic spectrum compatible seismic records of Bingol, Friuli and Loma Prieta (for the first checking) and Imperial Valley and Parkfield (for verification). The same seismic records are also made compatible with the ULS elastic spectrum for an additional verification. These physical seismic records are made spectrum compatible by using a special software (Karabalis *et al.* 1994).

Figs. 2 and 3 show the seismic drifts and storey and total damage, respectively, of frame F for all five seismic records for the $x + 0.3z$ loading combination and the DLS. Tables 3 and 4 provide member damage indices and plastic rotations, respectively, for all five seismic records for the $x + 0.3z$ loading combination and the DLS. Only the first two most highly stressed members are shown in the tables. It is observed that all storeys develop seismic drifts higher than those of the $\pm$ 0.05 L_i accidental eccentricity case (Vasilopoulos and Beskos 2008) but still lower than the DLS limit of 1.50%h = 0.015 × 3.20 = 4.80 cm. It is observed that damage at member, storey and structural level, eventhough increased in comparison to that of the $\pm$ 0.05 L_i accidental eccentricity case (Vasilopoulos and Beskos 2008), remains less than or equal to the DLS limit of 20%. Plastic hinge rotations have also been increased in comparison to the

Table 3 Member damage indices for frame F ($x + 0.3z$ / DLS)

Bingol		
Member	*i*-end damage	*j*-end damage
No Damage		
Friuli		
Member	*i*-end damage	*j*-end damage
45	12.09%	11.95%
52	11.93%	11.98%
Impo		
Member	*i*-end damage	*j*-end damage
45	11.86%	8.91%
52	10.41%	11.83%
LomP		
Member	*i*-end damage	*j*-end damage
42	11.92%	6.80%
44	3.87%	11.83%
Parko		
Member	*i*-end damage	*j*-end damage
74	11.87%	7.82%
81	10.02%	11.84%

Table 4 Plastic hinge rotations for frame F ($x + 0.3z$ / DLS)

Bingol		
Member	*i*-end rot	*j*-end rot
No plastic rotation		
Friuli		
Member	*i*-end rot	*j*-end rot
45	4.52355	4.0941
52	4.2082	4.366
Impo		
Member	*i*-end rot	*j*-end rot
45	4.102	3.67095
52	3.78555	3.9397
LomP		
Member	*i*-end rot	*j*-end rot
13	4.8947	3.708
42	5.123	4.0953
Parko		
Member	*i*-end rot	*j*-end rot
42	4.7331	3.7987
71	4.72645	3.6472

accidental eccentricity case (Vasilopoulos and Beskos 2008), but are still lower than the DLS limit of $\theta_{pl} / \theta_y = 6$. It has also been found from the analyses that plastic hinges develop only in beams in accordance with the capacity design criterion (Vasilopoulos and Beskos 2005).

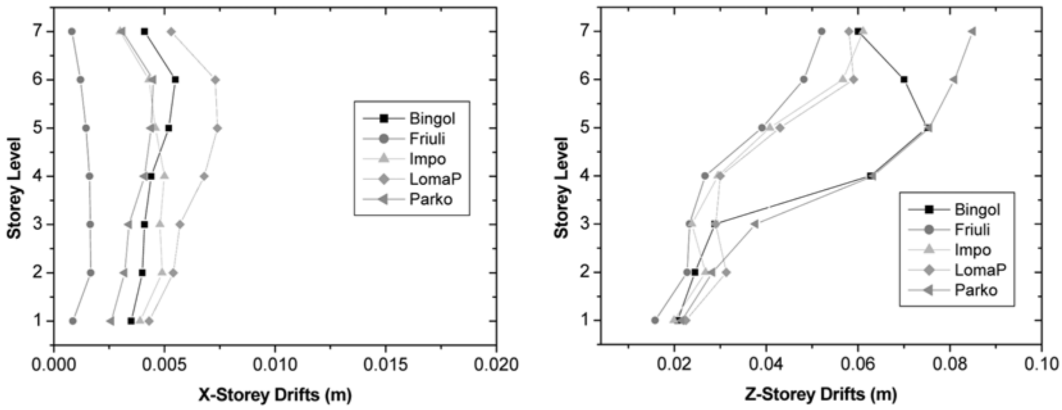

Fig. 4 Seismic drifts of frame F for all five seismic records ($z + 0.3x$ / DLS)

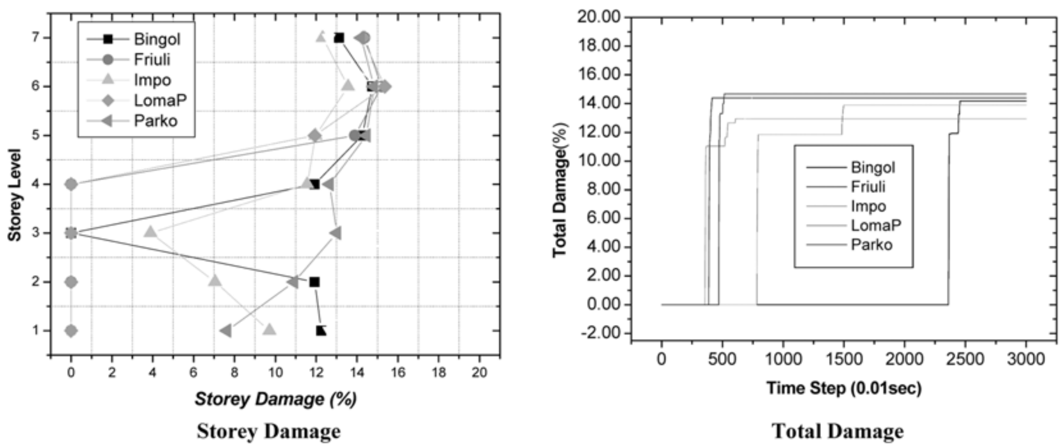

Fig. 5 Storey and total damage of frame F for all five seismic records ($z + 0.3x$ / DLS)

Figs. 4 and 5 and Tables 5 and 6 present analogous results as before for the $z + 0.3x$ loading combination and the DLS. Only the first two most highly stressed members are shown in the tables. It is observed that seismic drifts are higher than those of accidental eccentricity case (Vasilopoulos and Beskos 2008) and that the ones along the z direction greatly exceed the DLS limit value of 4.80 cm. Damage at member, storey and structural level shows a small increase in comparison with that of the accidental eccentricity case (Vasilopoulos and Beskos 2008) but remains smaller than the DLS limit of 20%. Plastic hinge rotations are higher than those in Vasilopoulos and Beskos (2008) but they remain smaller than the DLS limit of $\theta_{pl} / \theta_y = 6$. It has also been found from the analyses that plastic hinges develop only in beams in accordance with the capacity design criterion (Vasilopoulos and Beskos 2005). Thus, frame F with eccentricities $\pm$ 0.15 L_i at each floor does not satisfy all the DLS criteria and some of its members have to become stronger.

Thus a frame F$'$ with HEB450, HEB400 and HEB360 columns for the first three, intermediate two and upper two storeys, respectively, weak axis beams the same as those of frame F and strong axis beams IPE270 and IPE200 for the first four and upper three storeys, respectively, was found to be the

Table 5 Member damage indices for frame F ($z + 0.3x$ / DLS)

Bingol		
Member	*i*-end damage	*j*-end damage
171	15.42%	15.41%
193	15.45%	15.15%
Friuli		
Member	*i*-end damage	*i*-end damage
164	15.82%	15.76%
171	15.82%	15.82%
Impo		
Member	*i*-end damage	*i*-end damage
164	15.37	15.30
171	15.37	15.36
LomP		
Member	*i*-end damage	*j*-end damage
164	15.65%	15.59%
171	15.66%	15.65%
Parko		
Member	*i*-end damage	*j*-end damage
164	16.00%	16.00%
171	15.93%	16.00%

Table 6 Plastic hinge rotations for frame F ($z + 0.3x$ / DLS)

Bingol		
Member	*i*-end rot	*j*-end rot
26	4.2098	4.8531
55	4.289	4.76965
Friuli		
Member	*i*-end rot	*j*-end rot
164	5.1642	5.0285
192	4.9607	4.0244
Impo		
Member	*i*-end rot	*j*-end rot
19	3.9157	3.70115
26	3.6379	4.24875
LomP		
Member	*i*-end rot	*j*-end rot
164	4.8668	4.7305
193	4.8622	4.2424
Parko		
Member	*i*-end rot	*j*-end rot
77	4.8836	4.5924
84	4.44025	5.0585

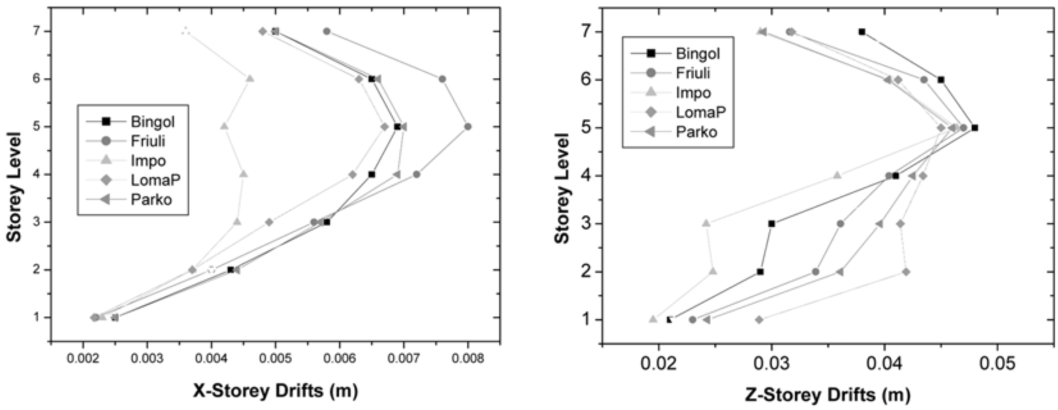

Fig. 6 Seismic drifts of frame F′ for all five seismic records ($z + 0.3x$ / DLS)

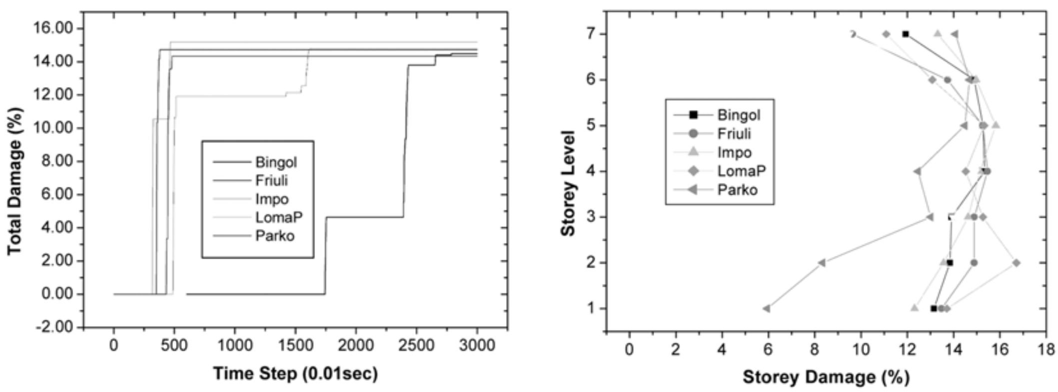

Fig. 7 Total and storey damage indices of frame F′ for all five seismic records ($z + 0.3x$ / DLS)

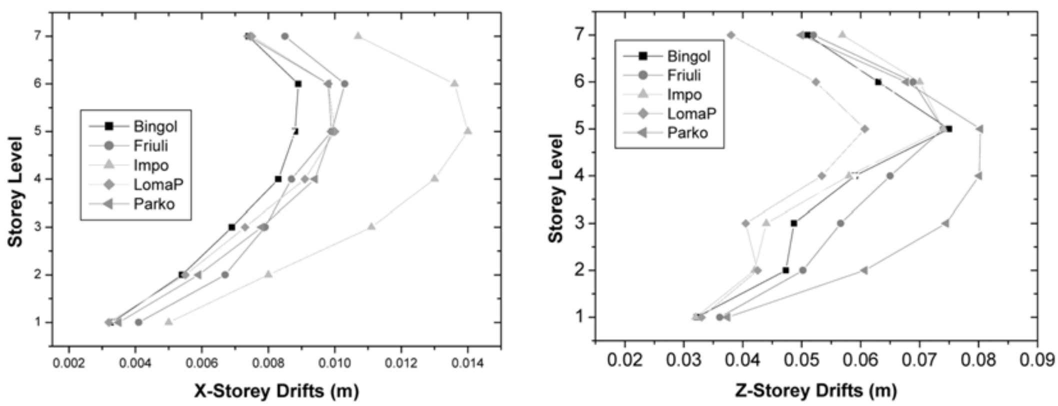

Fig. 8 Seismic drifts of frame F′ for all five seismic records ($z + 0.3x$ / ULS)

best solution. Indeed, as Figs. 6 and 8 for the seismic drifts due to the $z + 0.3x$ seismic load combination show, the maximum drifts along the z direction are very close to but do not exceed the limit values of

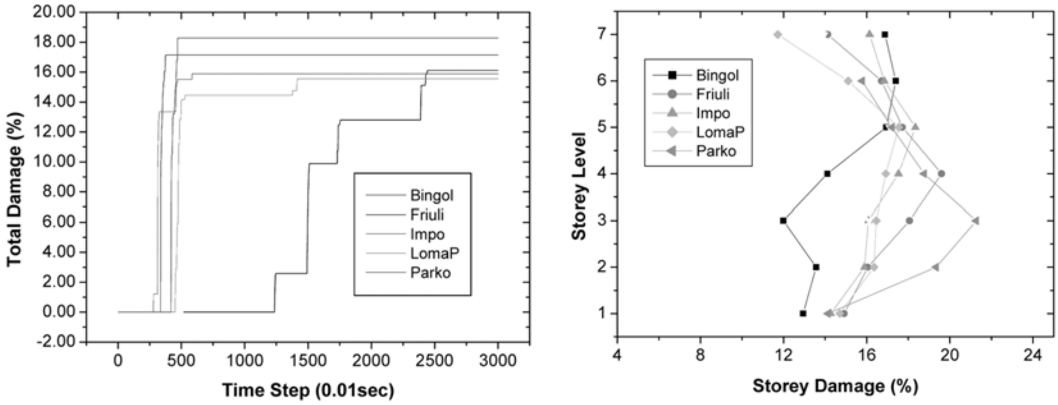

Fig. 9 Storey and total damage indices of frame F′ for all five seismic records ($z + 0.3x$ / ULS)

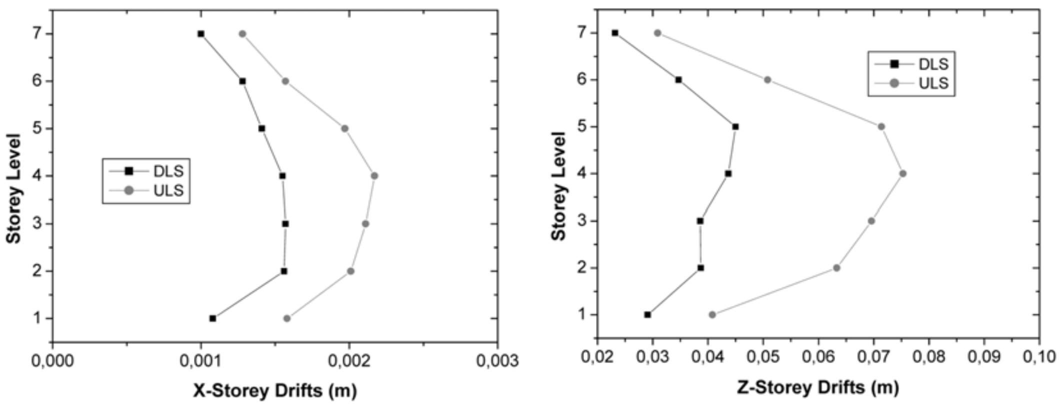

Fig. 10 Seismic drifts of frame F′ from pushover analysis for the DLS and ULS ($z + 0.3x$)

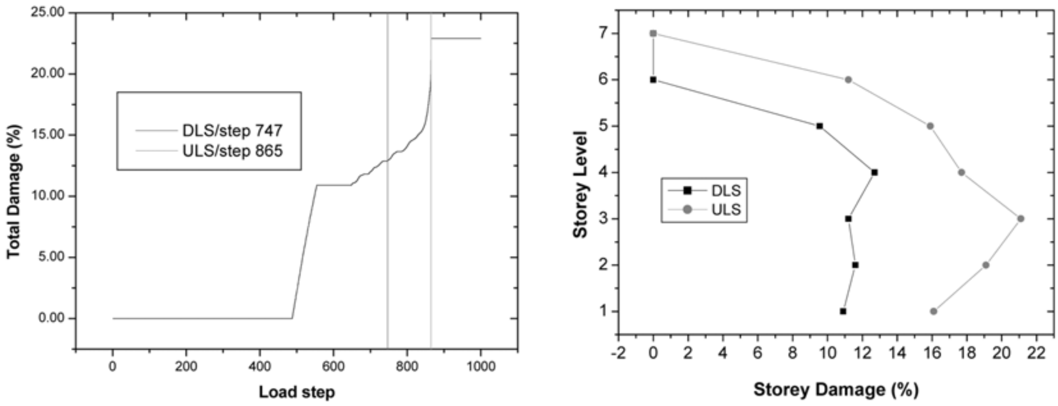

Fig. 11 Total and storey damage indices of frame F′ from pushover analysis for the DLS and ULS ($z + 0.3x$)

1.50% × 320 = 4.80 cm and 3.0% × 320 = 9.60 cm for the DLS and ULS, respectively. Furthermore, as Figs. 7 and 9 for the storey and total damage indices show, damage does not exceed the limit values of

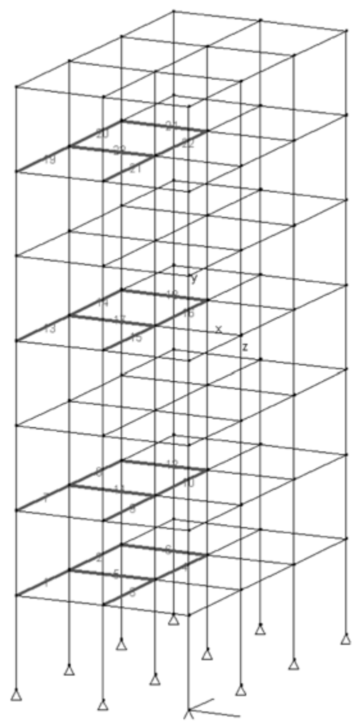

Fig. 12 (a) Seven storey space steel frame F′ with considered beams

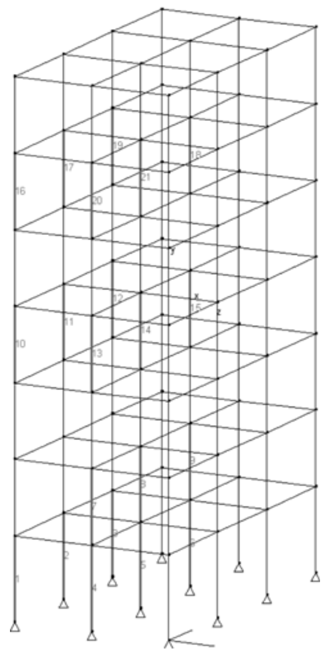

Fig. 12 (b) Seven storey space steel frame F′ with considered columns

20% and 50% for the DLS and ULS, respectively. The same is true for the member damage indices not shown here for lack of space (Vasilopoulos and Beskos 2005). Finally, plastic rotations and plastic hinge formation patterns, not shown here due to space limitations, also satisfy the corresponding DLS and ULS requirements (Vasilopoulos and Beskos 2005). A serviceability check was also made with respect to drifts, which were found to be less than the limit value of 0.5% × 320 = 1.60 cm.

The best solution represented by Frame F′ is also tested on the basis of pushover analyses. Fig. 10 shows the seismic drifts for the load combination $z + 0.3x$ for the DLS and ULS and clearly indicates that their maximum values of 4.50 cm and 7.50 cm for the DLS and ULS, respectively, are smaller than the corresponding limit values of 4.80 cm and 9.60 cm. Fig. 11 provides total and storey damage indices for the load combination $z + 0.3x$ and the DLS and ULS and clearly indicates that damage does not exceed the corresponding limit values (12.50% for DLS and 23.00% for ULS). One can also prove that all remaining requirements of the DLS and ULS are satisfied thereby confirming that Frame F′ represents the best solution (Vasilopoulos and Beskos 2005). Furthermore, one can also find from pushover analyses that the inelastic base shears along the strong axes of the frame have the values of V_p^z = 1610 kN and V_p^x = 590 kN, respectively. Dynamic spectral analysis (q = 1.0, pga = 0.30 g, soil class B and damping ξ = 5.0%) gives V_{el}^z = 4950 kN and V_{el}^x = 2105 kN. Thus, the corresponding base shear ratios V_{el}^z / V_p^z

Table 7 Design/strength (capacity) ratios of beams of seven storey space steel frame according to EC3

Member	Section Strength	Member Strength
	Biaxial Bending + Shear + Axial Force	Lateral Torsional Buckling
1	0.215	0.427
2	0.138	0.395
3	0.455	0.844
4	0.287	0.786
5	0.784	
6	0.758	0.703
7	0.412	
8	0.247	0.464
9	0.768	
10	0.455	0.944
11	0.864	0.844
12	0.852	0.731
13	0.503	
14	0.275	
15	0.906	
16	0.488	1.004
17	0.738	0.867
18	0.735	0.858
19	0.180	0.387
20	0.102	0.342
21	0.298	0.839
22	0.223	0.775
23	0.978	0.244
24	0.984	

Table 8 Design/strength (capacity) ratios of columns of seven storey space steel frame according to EC3

Member	Section Strength	Member Strength	
	Biaxial Bending + Shear + Axial Force	Flexural Buckling	Lateral Torsional Buckling
1	0.345	0.546	0.557
2	0.716	0.959	0.971
3	0.713	0.955	0.967
4	0.427	0.796	0.818
5	0.856	0.296	0.318
6	0.852	0.292	0.313
7	0.362	0.643	0.649
8	0.572	0.898	0.905
9	0.569	0.894	0.901
10	0.114	0.227	0.230
11	0.272	0.467	0.472
12	0.271	0.466	0.470
13	0.134	0.331	0.337
14	0.373	0.668	0.677
15	0.372	0.666	0.676
16	0.205	0.271	0.273
17	0.436	0.557	0.560
18	0.433	0.553	0.556
19	0.290	0.406	0.410
20	0.596	0.791	0.798
21	0.591	0.786	0.793

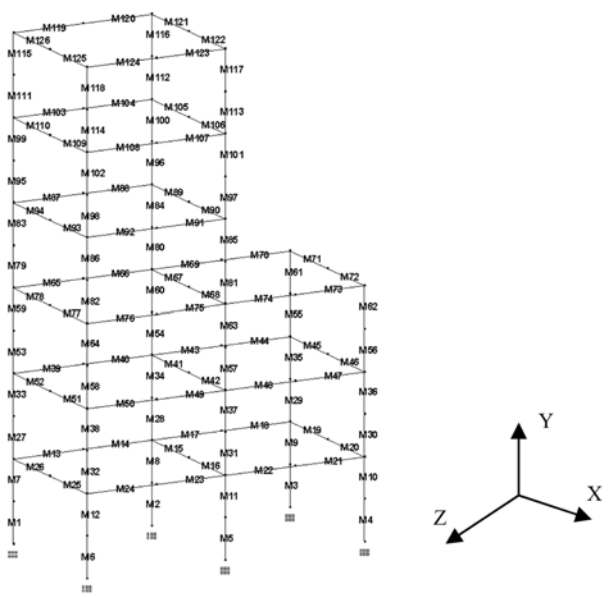

Fig. 13 Geometry and finite element numbering of vertically irregular frame

= 3.07 and V_{el}^{x}/V_{p}^{x} = 3.56 are rather close and between the values of 3 and 4, meaning that the structure is properly designed.

Finally, for comparison purposes, the commercial program SAP2000 (1997) is also used for the seismic design of the seven storey frame considered here in accordance with EC 8 (2004) and EC 3 (1992) codes. The behavior factor q was taken to be 4. Tables 7 and 8 provide the values of the design/strength (capacity) ratios of EC 3 (1992) under various states of deformation corresponding to beams and columns of frame F′ with numbering that shown in Figs. 12(a),(b). It is observed that frame F′ represents again the best design solution as the capacity ratios approach 1.00 without exceeding it.

5.2 Six storey space steel frame with a setback

Consider the irregular six storey space steel frame of Fig. 13. The frame has one and two bays along the x and z directions, respectively. The upper three storeys of the frame have only one bay along the z direction. This frame is known in the literature as the Orbison (1982) building. The height of every storey is 3.658 m, while the bay openings everywhere are 7.315 m. Beams have IPE sections and columns HEB sections. The grade of steel is S275. The frame is founded on soil class B. The modulus of elasticity E and shear modulus G of steel are 205 GPa and 85.4 GPa respectively, while strain hardening equals 3.0%. The frame damping ξ = 5.0%

The weight density of structural members γ_s = 78.50 kN/m^3 and the concrete slab and secondary beams self weight G_{s1} = 4.00 kN/m^2, the weight of upholsteries and floors G_{s2} = 1.50 kN/m^2, the weight of the light partition walls G_{w1} = 0.50 kN/m^2, the weight of the exterior glass panels G_{w2} = 2.00 kN/m^2, the rest dead type of weight due to mechanical networks, etc G_v = 1.00 kN/m^2 and the live loads Q = 3.00 kN/m^2. According to EC 8 (2004), the effective seismic mass is defined as $G_{tot} + 0.3Q$ and placed at the mass center of each floor.

Due to the diaphragm action in each floor slab, there are three degrees of freedom at the center of each floor: two horizontal translations (along the x and z axes) and one rotation (about the y axis). In this frame, there are no real in-plan eccentricities at each floor. Thus, in accordance with EC 8 (2004), accidental eccentricities equal to 0.05 L_i, where L_i is the width of the floor slab perpendicular to the direction of the considered motion, are taken into account. The effect of accidental eccentricities is taken into account by equivalent diaphragmatic torsional moments for the case of pushover analysis and by displacing the center of mass of each diaphragm for the case of dynamic nonlinear analysis.

The lateral seismic forces for both types of analysis are applied, according to EC 8 (2004), simultaneously along both x and z directions following the $x + 0.3z$ and $z + 0.3x$ rule in conjunction with the corresponding accidental eccentricities $\pm$ 0.05 L_i Thus, four different analyses are performed for each type (dynamic and pushover) of analysis. The dynamic nonlinear analyses are performed by using the five elastic spectrum compatible seismic records of the previous example for the two limit states of DLS and ULS.

For both types of analyses the design process is iterative starting with an original section selection

Table 9 Member sections of the Orbison frame

Frame	Sections
A	HEB360/340/320/300 (columns) - IPE300/270/240 (beams)
B	HEB400/360/340/320 (columns) - IPE330/300/270 (beams)
C	HEB450/400/360/320 (columns) - IPE360/330/300/270 (beams)
D	HEB500/450/400/360 (columns) - IPE400/360/330 (beams)

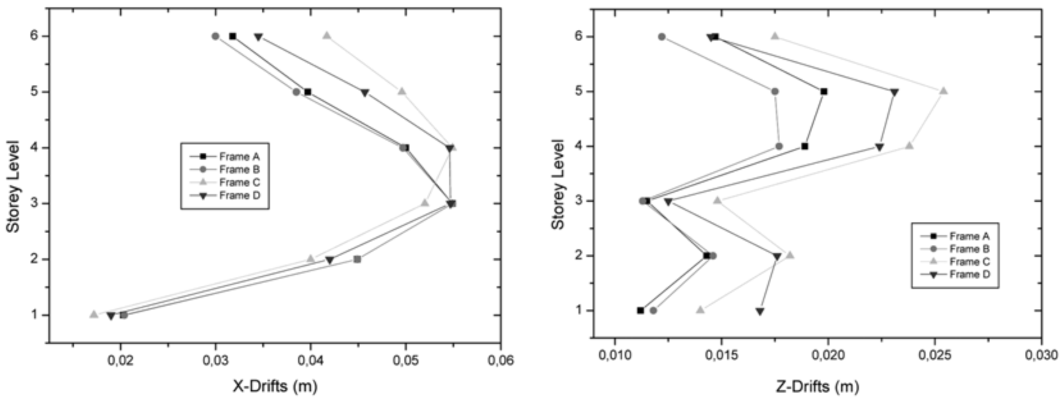

Fig. 14 Lateral storey drifts from pushover analyses (x + 0.3z / DLS)

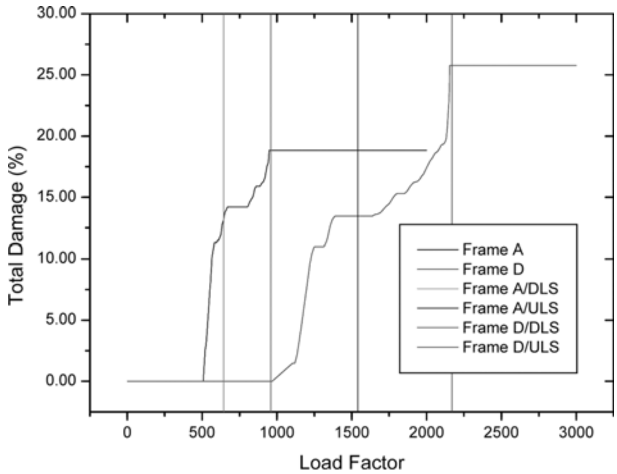

Fig. 15 Total damage indices from pushover analyses (x + 0.3z / DLS and ULS)

Table 10 Member damage indices from pushover analyses (x + 0.3z / DLS)

Orbison frame A				Orbison frame D			
Member No	Damage Start	*i*-end Damage	*j*-end Damage	Member No	Damage Start	*i*-end Damage	*j*-end Damage
52	508		15.15%	51	1126	16.48%	
78	526		14.28%	78	1100		16.26%

(frame A of Table 9) and arriving at the final optimum section selection (frame D of Table 9). Concerning the columns in Table 9, the first number corresponds to the first two storeys, the second number to the third storey, the third number to the fourth and fifth stories and the fourth number to the sixth storey. Concerning the beams in Table 9, for frame A the first number corresponds to the first two floors, the second number to the next three floors and the third number to the sixth floor, while for frame D the first two numbers correspond to the first two floors, the second number to the third floor and the third number to the last three floors. Due to space limitations, only partial results concerning

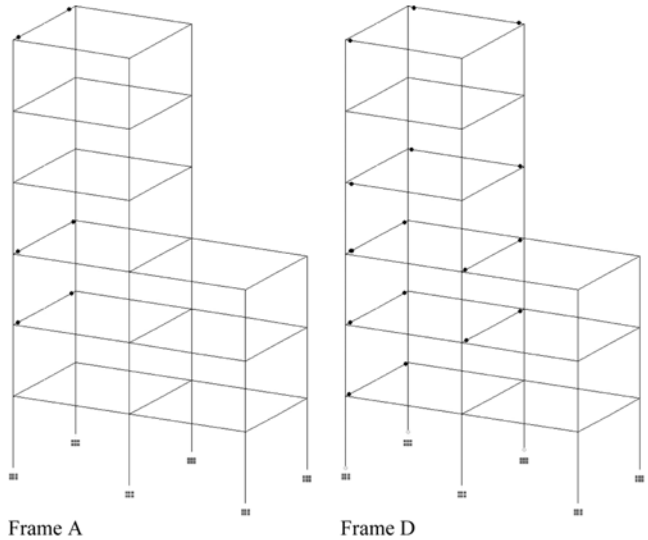

Fig. 16 Plastic hinge formation from pushover analyses (x + 0.3z / DLS)

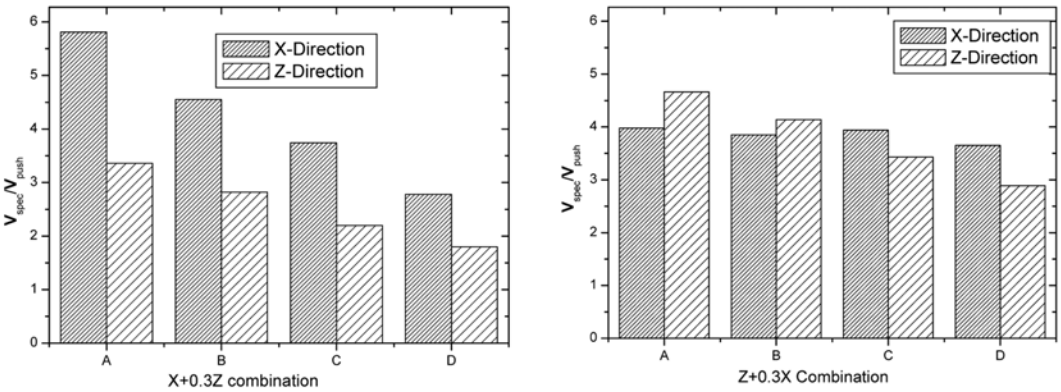

Fig. 17 Ratios of spectral(elastic) base shear over pushover(plastic) base shear for DLS

frames A and D are presented here. More details can be found elsewhere (Vasilopoulos and Beskos 2005).

Results from the design process based on pushover analysis are presented first. Consider first frame A for the case x + 0.3z/DLS. Fig. 14 provides the seismic drifts along the x and z directions. The maximum drift value of 5.49 cm, observed along the z direction at the third floor, does not exceed the limit value 1.5% × 365.8 = 5.49 cm of Table 2. Fig. 15 depicts the total damage index versus lateral load factor, which attains a maximum value of 13.80%. Storey damage indices (not shown here) attain a maximum value of 14.68% for the second floor, while member damage indices shown in Table 10 attain a maximum value of 16.48%. Thus, damage indices do not exceed the limit value 20.00% of Table 1. Fig. 16 shows that plastic hinges appear only in beams thereby satisfying the capacity design criterion of Table 1. The x direction design base shear from pushover analysis was found to be $V_{in}^{x} = 288.10\ \mathrm{kN}$, while the x direction elastic base shear from spectral analysis with q = 1 was found to be $V_{el}^{x} = 1676.64\ \mathrm{kN}$ Thus, the ratio $V_{el}^{x}/V_{p}^{x} = 5.81$ as shown in Fig. 17. Similarly, $V_{el}^{z}/V_{p}^{z} = 3.36$ again as shown in Fig. 17. In conclusion, one can observe that while all the criteria of Table 2 are satisfied for frame A, the ratios $V_{el}/$

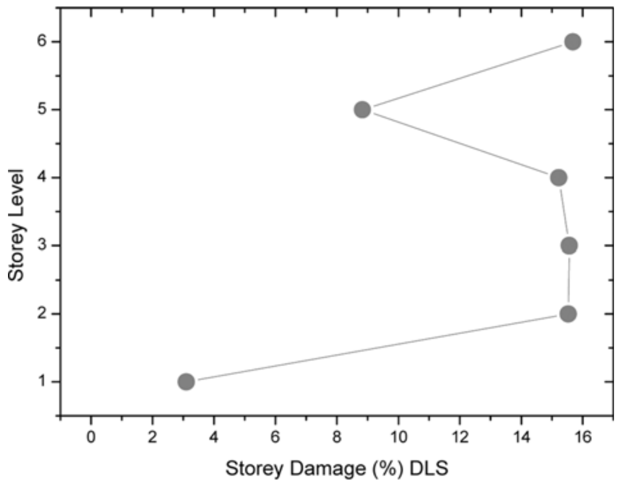

Fig. 18 Storey damage indices of frame D from pushover analyses (x + 0.3z / DLS)

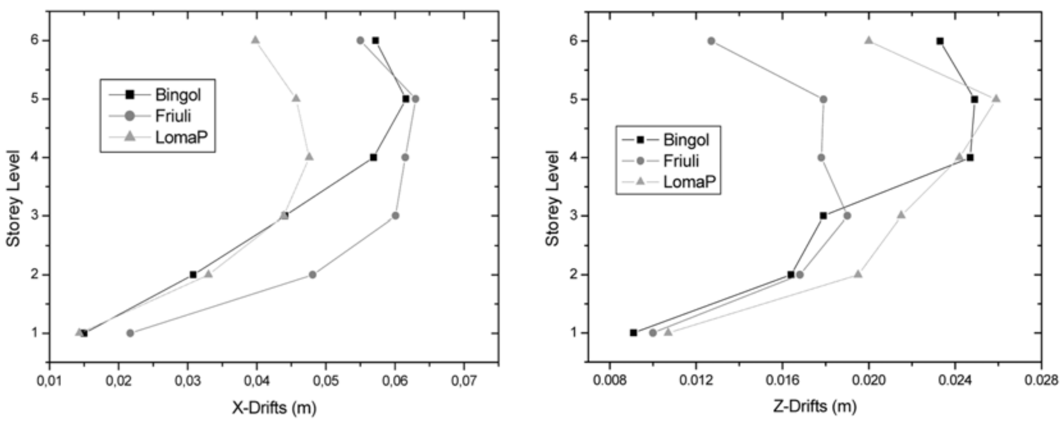

Fig. 19 Seismic storey drifts of frame A from dynamic analyses (x + 0.3z / DLS)

V_p along the two directions do not both approach the values 3 or 4 (one of them is 5.81) indicating that frame A is underdesigned. Analogous conclusions can be reached for the $z + 0.3x$ load combination (Vasilopoulos and Beskos 2005).

Figs. 14~18 and Table 10 present response results (drifts, member, storey and total damage indices and plastic hinge formation pattern) for the x + 0.3z load combination for the DLS of frame D. Only the first two most highly stressed members are shown in Table 10. It is apparent that all these response values do not exceed the allowable DLS limits of Table 1 (e.g. total damage D = 13.50%), while plastic hinges are formed only in beams. Furthermore, as Fig. 17 shows, the ratio V_{el}/V_p attains the values of 2.70 and 1.80 along the x and z direction, respectively. Analogous conclusions can be drawn for the $z + 0.3x$ load combination (Vasilopoulos and Beskos 2005). In particular, as Fig. 17 shows, the ratio V_{el} / V_p for the $z + 0.3x$ load combination attains the values 3.60 and 2.90 along the x and z direction, respectively. Thus, it appears that frame D presents the best section selection since, as shown in Fig. 17, the values of the V_{el}/V_p ratio are closer to each other and around the value of 3 than in any of the other cases (frames A, B and C of Table 9).

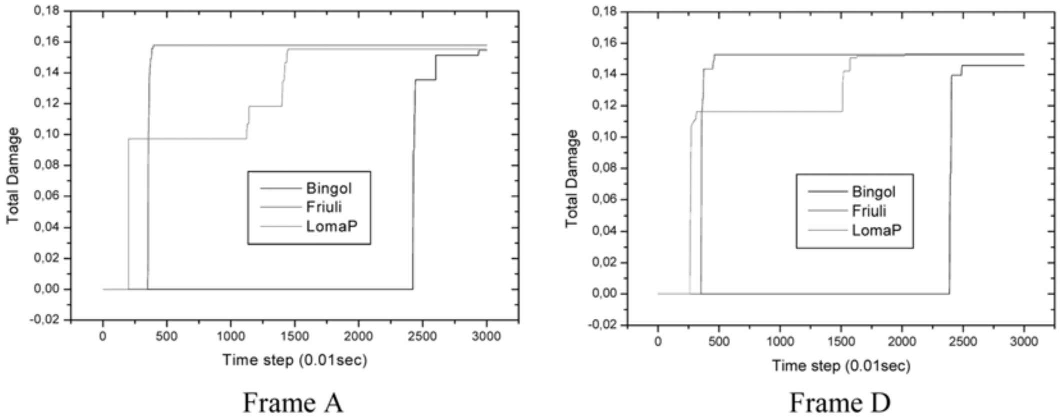

Fig. 20 Total damage indices from dynamic analyses ($x + 0.3z$ / DLS)

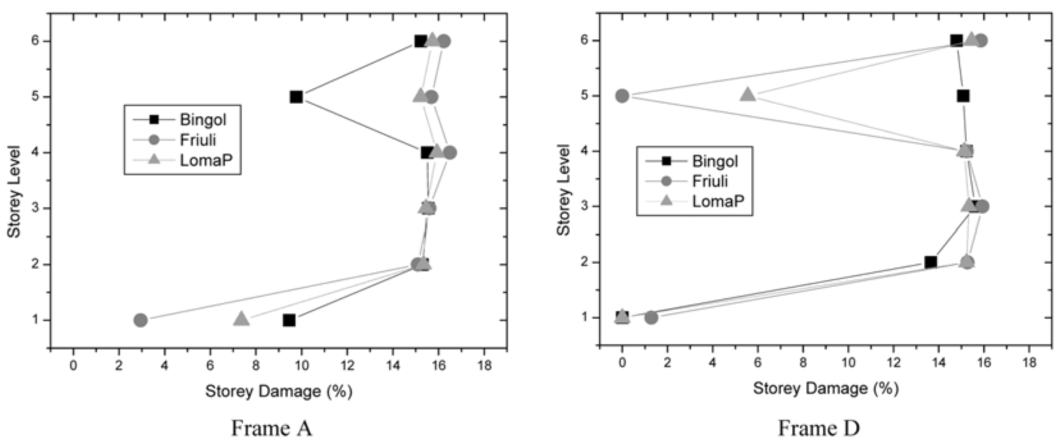

Fig. 21 Storey damage indices from dynamic analyses ($x + 0.3z$ / DLS)

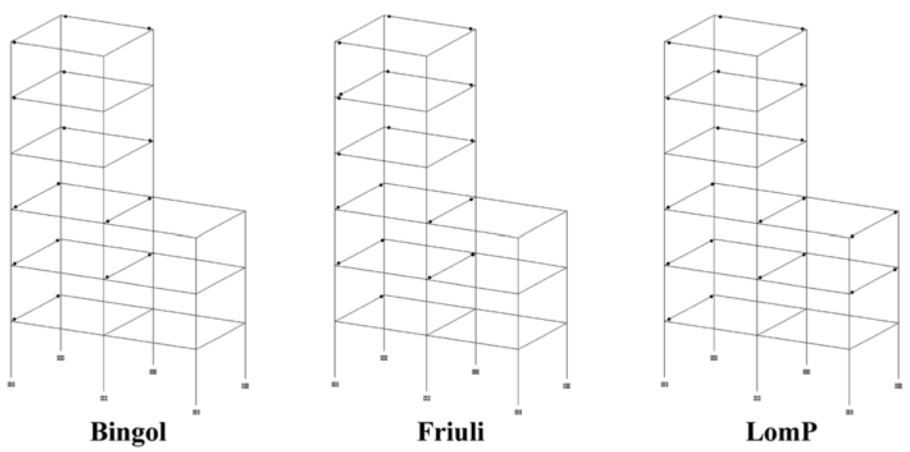

Fig. 22 Seismic plastic hinge formation of frame A from dynamic analyses ($x + 0.3z$ / DLS)

Table 11 Member damage indices from dynamic analyses ($x + 0.3z$ / DLS)

Orbison frame A / Bingol			
Member No	Damage Start	*i*-end Damage	*j*-end Damage
78	2433	15.60%	
91	2447	15.50%	
Orbison frame A / Friuli			
Member No	Damage Start	*i*-end Damage	*j*-end Damage
87	370	17.10%	
119	364	16.40%	
Orbison frame A / LomP			
Member No	Damage Start	*i*-end Damage	*j*-end Damage
87	1407	16.90%	
119	1393	16.50%	

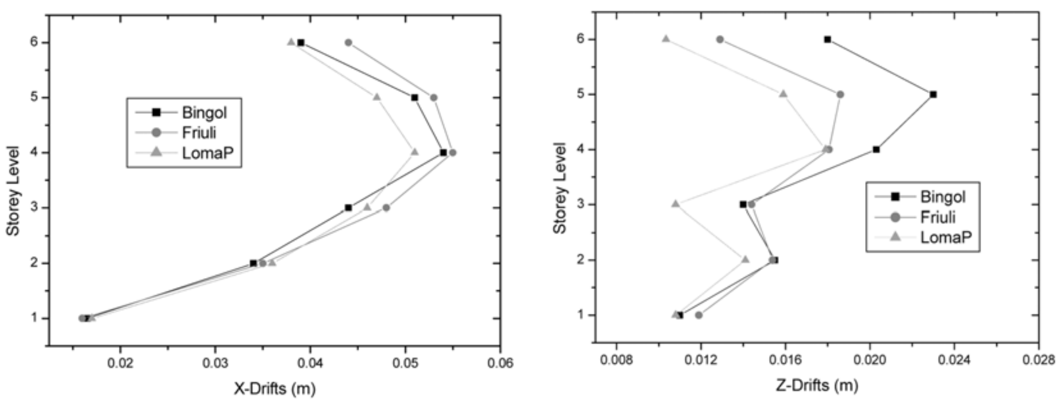

Fig. 23 Seismic storey drifts of frame D from dynamic analyses ($x + 0.3z$ / DLS)

One can also find out (Vasilopoulos and Beskos 2005) that pushover response results for frame D under both the $x + 0.3z$ and $z + 0.3x$ load combinations for the ULS exhibit maximum values in agreement with the restrictions set up in Table 2. Thus, for example, drifts approach the allowable limit of 3.0% h = 3.0% × 365.8 = 10.97 cm, damage indices reach a maximum value of 26.00% (total damage from Fig. 15), much lower than the limit of 50% and plastic hinges appear not only in beams but in columns as well. A serviceability check was also made with respect to drifts, which were found to be less than the limit value of 0.5% × 365.8 = 1.83 cm.

Results from the design process based on dynamic nonlinear analysis are presented in the following. Consider first frame A of Table 9 under the DLS spectrum compatible seismic records of Bingol, Friuli and Loma Prieta applied in turn in accordance with the $x + 0.3z$ load combination. Figs. 19~22 and Table 11 present seismic response results in terms of drifts, member, storey and total damage indices and plastic hinge formation pattern. Only the first two most highly stressed members are shown in Table 11. It is observed that the maximum value 6.30 cm of drift occurring at the fifth floor (x direction) due to the Friuli earthquake exceeds the limit value of 1.5% h = 1.5% × 365.8 = 5.49 cm of Table 1, while the maximum values of damage indices 15.79% (total damage due to Friuli), 15.93% (storey damage at fifth floor due to Bingol) and 17.10% (member damage due to Friuli) do not exceed the limit value of

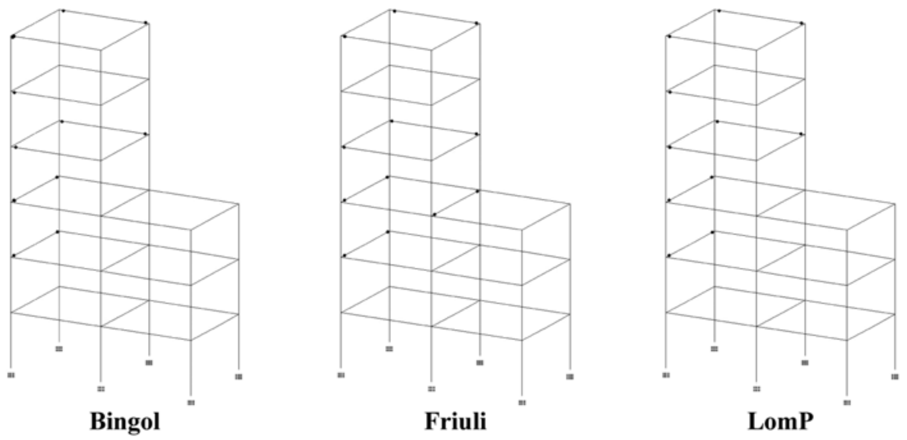

Fig. 24 Seismic plastic hinge formation of frame D from dynamic analyses ($x + 0.3z$ / DLS)

Table 12 Member damage indices from dynamic analyses ($x + 0.3z$ /DLS)

	Orbison frame D / Bingol		
Member No	Damage Start	*i*-end Damage	*j*-end Damage
87	2402	16.25%	
119	2412	15.94%	
	Orbison frame D / Friuli		
Member No	Damage Start	*i*-end Damage	j-end Damage
77	417	16.00%	
123	419	15.94%	
	Orbison frame D / LomP		
Member No	Damage Start	*i*-end Damage	*j*-end Damage
77	1032	15.46%	
78	1031		15.59%

20.00% of Table 1. It is also observed that plastic hinges develop only in beams. Analogous results are obtained for frame A under the $z + 0.3x$ load combination (Vasilopoulos and Beskos 2005). Thus, one can conclude that frame A is inadequate and its member sections have to be increased. The design proceeds with the checking of frames B, C and D of Table 6, until the best solution (frame D) is found.

Figs. 23, 20, 21 and 24 and Table 12 provide response results for frame D under the DLS spectrum compatible seismic records of Bingol, Friuli and Loma Prieta applied in turn in accordance with the $x + 0.3z$ load combination. Only the first two most highly stressed members are shown in Table 12. It is observed that the maximum value 5.50 cm of drift occurring at the third floor (x direction) due to the Friuli seismic motion slightly exceeds the limit value of 5.49 cm, while the maximum values of damage indices 15.32% (total damage due to Loma Prieta), 15.53% (storey damage at third floor due to Loma Prieta) and 16.25% (member damage due to Bingol) do not exceed the limit value of 20.00%. It is also observed that plastic hinges develop only in beams. Analogous results are obtained for frame D under the $z + 0.3x$ load combination (Vasilopoulos and Beskos 2005). Thus, one can conclude that frame D appears to be the best solution.

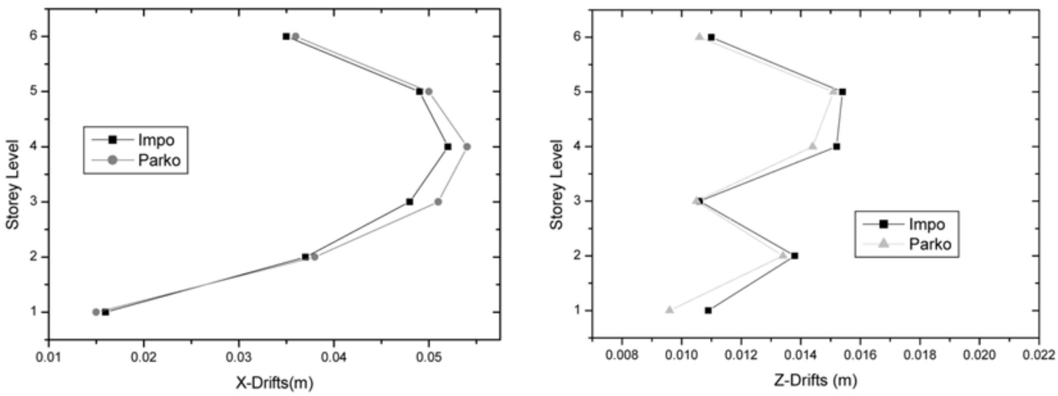

Fig. 25 Seismic storey drifts for frame D ($x + 0.3z$ / DLS)

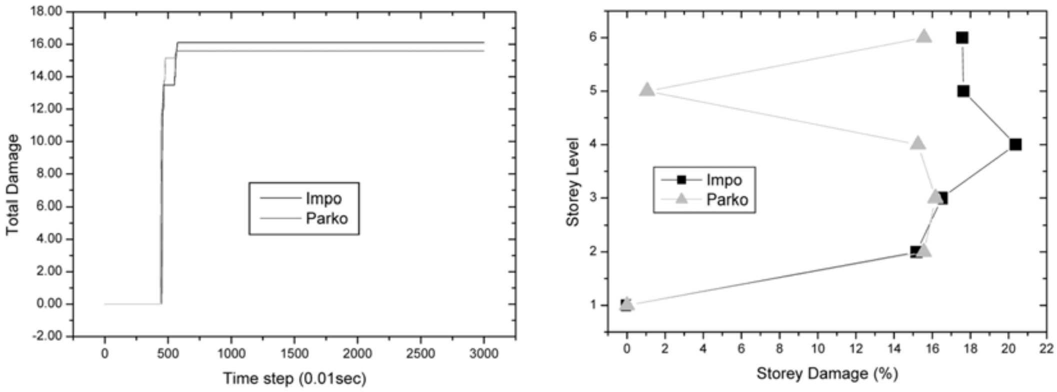

Fig. 26 Seismic total and storey damage indices for frame D ($x + 0.3z$ / DLS)

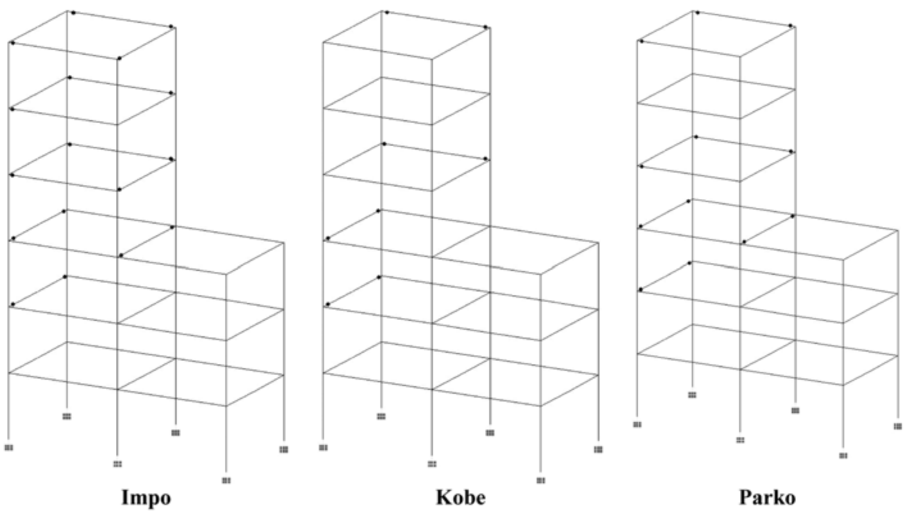

Fig. 27 Plastic hinge formation in frame D from seismic excitations ($x + 0.3z$ / DLS)

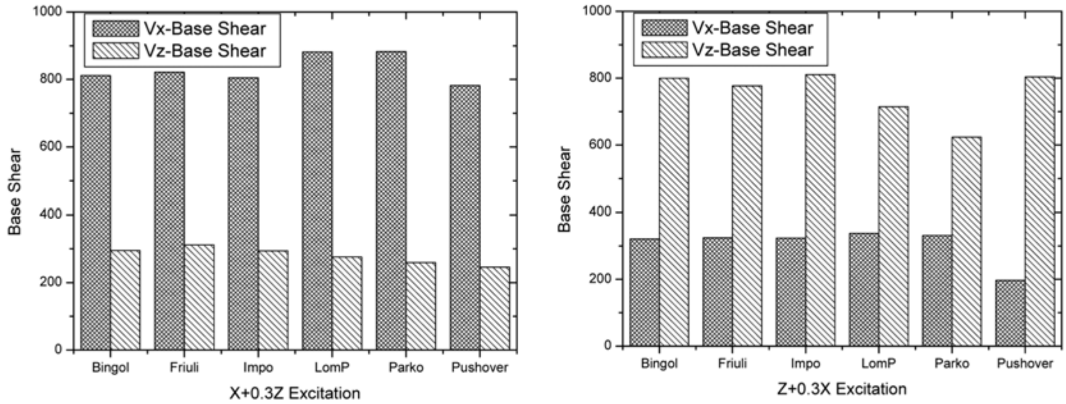

Fig. 28 Base shear values from dynamic and pushover analyses of frame D (DLS)

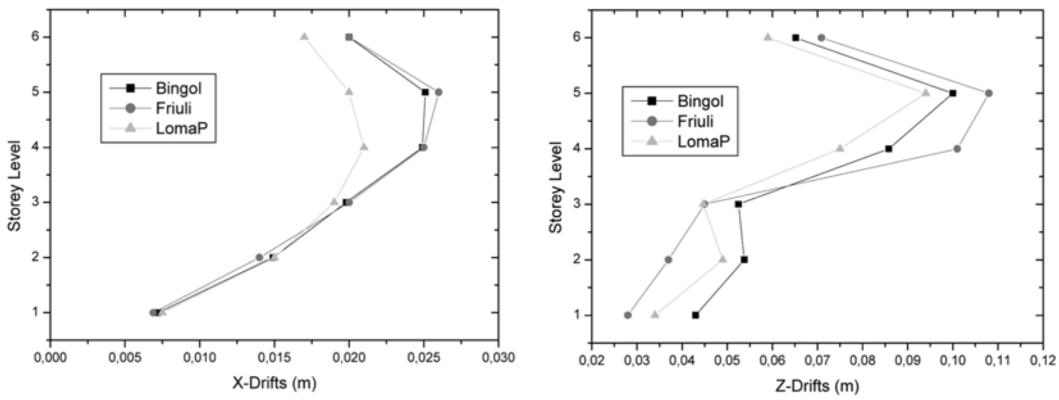

Fig. 29 Seismic storey drifts for frame D ($z + 0.3x$ / ULS)

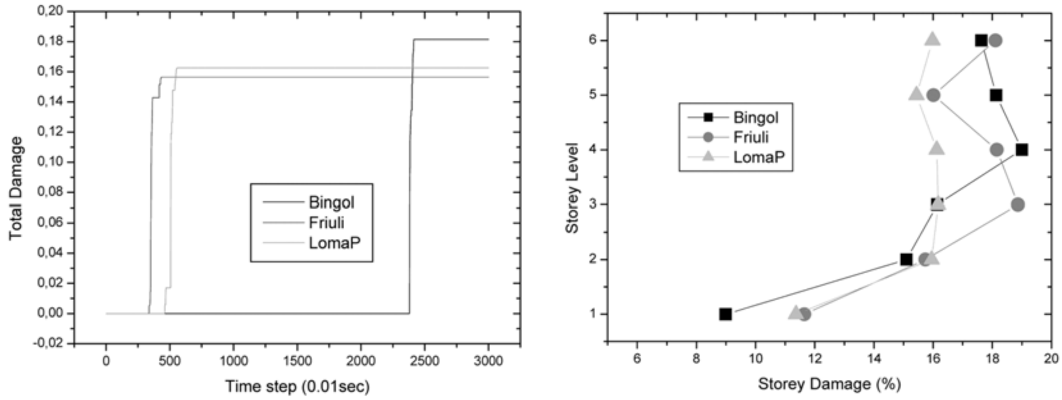

Fig. 30 Seismic total and storey damage indices for frame D ($x + 0.3z$ / ULS)

A further verification of the best solution (frame D) is done by performing additional dynamic analyses for both load combinations $x + 0.3z$ and $z + 0.3x$ and seismic input consisting of the DLS

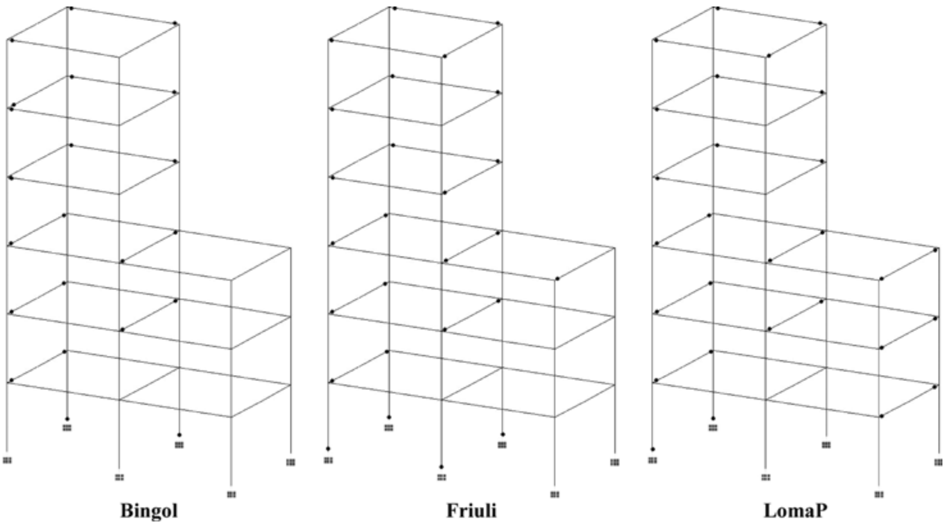

Fig. 31 Plastic hinge formation in frame D from seismic excitations (x + 0.3z / ULS)

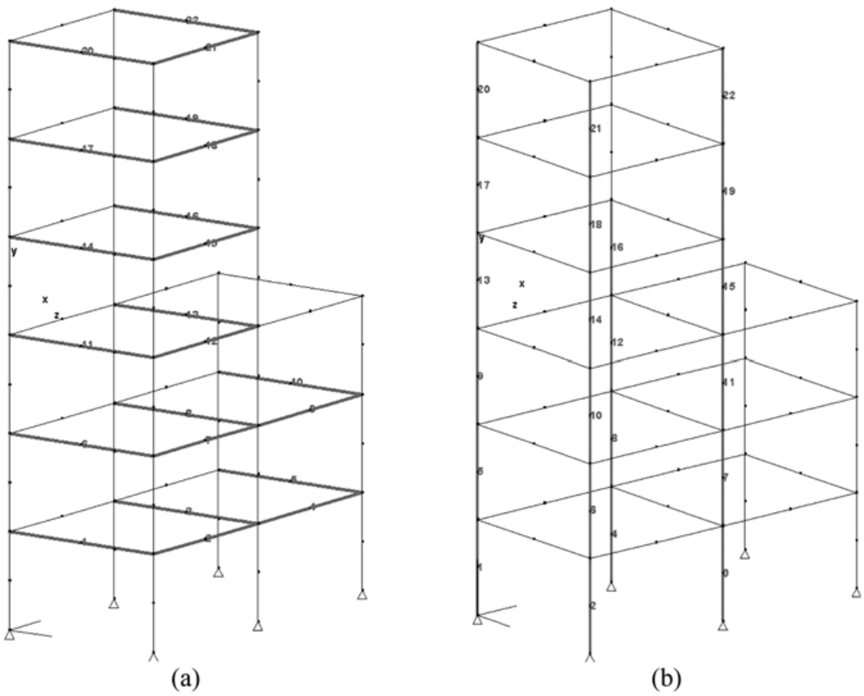

Fig. 32 Orbison frame D with considered beams (a) and columns (b)

spectrum compatible earthquakes of Imperial Valley and Parkfield. Figs. 25~27 provide some response results (for more see also Vasilopoulos and Beskos 2005) in terms of drifts, damage and plastic hinge formation pattern and verify that frame D is indeed the best solution. To be sure, the maximum seismic storey drift in Fig. 25 and the maximum storey damage in Fig. 26 slightly exceed the corresponding limit values (5.50 > 5.49 cm and 20.20% > 20.00%) for the DLS case but this is considered to be insignificant. This assertion is also supported by Fig. 28, which provides the maximum values of base shears along the x and z directions as obtained by the dynamic and static (pushover) nonlinear analyses for both load combinations $x + 0.3z$ and $z + 0.3x$. It is observed that the results are in satisfactory agreement, especially those of the dynamic analyses.

An additional checking of the seismic performance of frame D in accordance with the proposed methodology is done with the aid of dynamic nonlinear analyses involving all five previously used seismic records in their form of ULS spectrum compatible. This compatibility is achieved by amplifying the elastic design spectrum of EC 8 (2004) by 1.5 and making all these seismic records compatible to the resulting ULS design spectrum with the aid of the special software of Karabalis *et al*. (1994). Figs. 29-31 show some response results in terms of drifts, damage and plastic hinge formation pattern for D under the load combination $x + 0.3z$ for the ULS. Additional results can be found in Vasilopoulos and Beskos (2005). It is observed that the maximum value of drifts (10.70 cm along z direction for $z + 0.3x$ combination) approaches without exceeding the ULS limit of 3.0% h = 3.0% × 365.8 = 10.97 cm, the maximum values of the total damage index approach the value of 20.00%, while those of the storey and member damage indices approach the value of 22% without though exceeding the limit of 50%. It is

Table 13 Design/strength (capacity) ratios of beams of Orbison frame D according to EC3

Member	Section Strength	Member Strength	
	Biaxial Bending + Shear + Axial Force	Flexural Buckling	Lateral Torsional Buckling
1		0.029	
2	0.417	1.025	
3		0.029	
4	0.416	1.023	
5		0.029	
6	0.010	0.015	
7	0.336	0.954	
8	0.008	0.016	
9	0.359	0.993	
10		0.030	
11	0.012	0.017	
12	0.444	1.083	
13	0.010	0.018	
14	0.012	0.030	
15	1.055	1.165	
16	0.011	0.030	
17		0.039	
18	0.817	1.125	
19		0.039	
20	0.018	0.028	
21	0.282	0.537	
22	0.018	0.028	

Table 14 Design/strength (capacity) ratios of columns of Orbison frame D according to EC3

Member	Section Strength	Member Strength	
	Biaxial Bending + Shear + Axial Force	Flexural Buckling	Lateral Torsional Buckling
1	0.596	0.844	0.844
2	0.596	0.843	0.844
3	0.638	1.032	1.032
4	0.638	1.032	1.033
5	0.369	0.573	0.573
6	0.369	0.573	0.573
7	0.602	0.868	0.869
8	0.602	0.869	
9	0.282	0.460	0.460
10	0.282	0.460	0.460
11	0.481	0.696	0.696
12	0.481	0.696	0.696
13	0.523	0.676	0.676
14	0.523	0.676	0.676
15	0.658	0.809	0.809
16	0.659	0.814	0.815
17	0.465	0.563	0.564
18	0.465	0.563	0.563
19	0.457	0.555	0.555
20	0.406	0.458	0.458
21	0.406	0.458	0.458
22	0.406	0.459	0.459

also observed that plastic hinges are formed not only in beams but in columns as well, without however leading to collapse. Thus, the ULS requirements are satisfied. A serviceability check was also made with respect to drifts, which were found to be less than the limit value of 0.5% × 365.8 = 1.83 cm.

The results of the proposed method of seismic design, i.e., the member section selection corresponding to frame D, are finally compared against those obtained by the well known analysis and design program SAP2000 (1997), which employs the design provisions of EC 8 (2004) and EC 3 (1992). The adequacy of frame D has been checked on the basis of the elastic design spectrum of EC 8 (2004) for soil B, damping 5.00%, peak ground acceleration (PGA) 0.30 g and behavior factor $q = 4$. The results of the design in the form of design / strength (capacity) ratios for various types of deformation are shown in Tables 13 and 14 for the most highly tressed beams and columns designated in Fig. 32. It is observed that frame D appears to be the best design from the EC 8 (2004) / EC 3 (1992) viewpoint as well.

6. Conclusions

On the basis of the developments in the previous sections, one can draw the following conclusions:

1. A rational and efficient seismic design methodology for irregular in-plan and elevation space steel

frames using advanced methods of analysis in the framework of EC 8/EC 3 has been presented.
2. These advanced methods of analysis are based on the finite element method incorporating material and geometric nonlinearities and can be of the static (pushover) or the dynamic type. Thus interaction of strength and stability between members of the structure can be taken into account in an exact and direct manner and use of the approximate behavior or buckling length factors is avoided.
3. According to the proposed methodology, the satisfaction or not of certain performance objectives dealing with drifts, plastic rotations, damage and pattern of plastic hinge formation and corresponding to certain performance levels is checked and the sections of the structural members are adjusted accordingly.
4. Irregular space frames in-plan or elevation are treated in a general, direct and unified way providing results, which eventhough similar to those of the EC 8/EC 3 approach, since the proposed method is calibrated against these codes, are at least obtained in a more rational and efficient way.

Acknowledgements

The authors acknowledge with thanks the assistance of Miss M. Dimitriadi in connection with the preparation of the manuscript.

References

Al-Ali, A. and Krawinkler, H. (1998), "Effects of vertical irregularities on seismic behavior of building structures", Rept No 130, John A Blume Earthquake Engineering Center, Stanford University, Stanford.

Chambers, J. and Kelly, T. (2004), "Nonlinear dynamic analysis-the only option for irregular structures", *In Proc. 13th World Conference on Earthquake Engineering*, Vancouver, B.C., Canada, August 1-6, Paper No 1389.

Chandler, A. M., Duan, X. N. and Rutenberg, A. (1996), "Seismic torsional response: assumptions, controversies and research progress", *Europ. Earthq. Eng.*, **10**, 37-51.

Chen, W. F. and Kim, S. E. (1997), *LRFD Steel Design Using Advanced Analysis*, CRC Press, Boca Raton, FL.

Chintanapakdee, C. and Chopra, A. K. (2004), "Seismic response of vertically irregular frames: response history and modal pushover analyses", *J. Struct. Eng., ASCE*, **130**, 1177-1185.

Chopra, A. K. and Goel, R. K. (2004), "A modal pushover analysis procedure to estimate seismic demands for unsymmetric-plan buildings", *Earthq. Eng. Struct. Dyn.*, **33**, 903-927.

De La Liera, J. and Chopra, A. K. (1995), "Understanding the inelastic seismic behavior of asymmetric plan buildings", *Earthq. Eng. Struct. Dyn.*, **24**, 549-572.

EC 3 (Eurocode 3) (1992), Design of Steel Structures, Part 1.1; General Rules for Buildings, European Prestandard ENV 1993-1-1/1992, European Committee for Standardization, Brussels.

EC 8 (Eurocode 8) (2004), Design of Structures for Earthquake Resistance-Part 1: General Rules, Seismic Actions and Rules for Buildings, EN 1998-1:2004, European Committee of Standardization (CEN), Brussels.

Ghobarah, A. (2001), "Performance-based design in earthquake engineering: state of development", *Eng. Struct.*, **23**, 878-884.

Gioncu, V. and Mazzolani F. M. (2002), *Ductility of Seismic Resistant Steel Structures*, Spon Press, London,

Humar, J. L. and Wright, E. W. (1977), "Earthquake response of steel framed multistorey buildings with setbacks", *Earthq. Eng. Struct. Dyn.*, **6**, 15-39.

Kappos, A. J. (2005), (ed.), *Proceedings of 4th European Workshop on the Seismic Behaviour of Irregular and Complex Structures*, 26-27 August, Thessaloniki, Greece (in CD-ROM format).

Kappos, A. J. and Manafpour A. (2001), "Seismic design of R/C buildings with the aid of advanced analytical

techniques", *Eng. Struct.*, **23**, 319-332.
Kappos, A. J. and Panagopoulos G. (2004), "Performance-based seismic design of 3D R/C buildings using inelastic static and dynamic analysis procedures", *ISET J. Earthquake Techn.*, **41**, 141-158.
Karabalis, D. L., Cokkinides, G. J., Rizos, D. C., Mulliken, J. S. and Chen, R. (1994), "An interactive computer code for generation of artificial earthquake records", *Comput. Civ. Eng.* (ASCE), Khozeimech K (ed.), New York, 1122-1155.
Kilar, V. and Fajfar, P. (2001), "On the applicability of pushover analysis to the seismic performance evaluation of asymmetric buildings", *Europ. Earthq. Eng.*, **15**, 20-31.
Kim, S. E. and Lee, J. (2002) "Improved refined plastic-hinge analysis accounting for lateral torsional buckling", *J. Constr. Steel Res.*, **58**, 1431-1453.
Marusic, D. and Fajfar, P. (2005), "On the inelastic seismic response of asymmetric buildings under bi-axial excitation", *Earthq. Eng. Struct. Dyn.*, **34**, 943-963.
Mazzolani, F. M. and Piluso, V. (1996), *Theory and Design of Seismic Resistant Steel Frames*, First edition, E&FN Spon, London.
NEHRP (1997), Guidelines for the Seismic Rehabilitation of Buildings, FEMA-273, Washington, D.C.
Orbison, J. K. (1982), "Nonlinear static analysis of three-dimensional steel frames", Report No 82-6, Department of Structural Engineering, Cornell University, Ithaca, New York.
Pavlidis, G., Bazeos, N. and Beskos, D. E. (2003), "Effects of higher modes and seismic frequency content on accuracy of pushover analysis of steel frames", In Mazzolani (ed.), *Behavior of Steel Structures in Seismic Areas, Proc. 4th Int. Conf. STESSA 2003*, Naples, Italy 2003; 547-550, Lisse, Holland: Swets & Zeitlinger.
Perus, I. and Fajfar, P. (2005), "On the inelastic torsional response of single-storey structures under bi-axial excitation", *Earthq. Eng. Struct. Dyn.*, **34**, 931-941.
Powell, G. H. and Allahabadi, R. (1988), "Seismic damage prediction by deterministic methods: concepts and procedures", *Earthq. Eng. Struct. Dyn.*, **16**, 719-734.
Prakash, V., Powell, G. H. and Campell, S. (1994), DRAIN-3DX, Base Program Description and User Guide, Version 1.10, Report No UCB/SEMM-94/08, University of California at Berkeley, August.
SAP 2000 (1997), Structural Analysis Program-Inelastic Version 7.44 Computers and Structures Inc., Berkeley, California.
Stathopoulos, K. G. and Anagnostopoulos, S. A. (2003), "Inelastic earthquake response of single-storey asymmetric buildings: an assessment of simplified shear-beam models", *Earthq. Eng. Struct. Dyn.*, **32**, 1813-1831.
Stathopoulos, K. G. and Anagnostopoulos, S. A. (2005), "Inelastic torsion of multistorey buildings under earthquake excitations", *Earthq. Eng. Struct. Dyn.*, **34**, 1449-1465.
Tremblay, R. and Poncet, L. (2005), "Seismic performance of concentrically braced steel frames in multistory buildings with mass irregularity", *J. Struct. Eng., ASCE* **131**, 1363-1375.
Tso, W. K. and Smith, R. S. (1999), "Re-evaluation of seismic torsional provisions", *Earthq. Eng. Struct. Dyn.*, **28**, 899-917.
UBC (Uniform Building Code) (1997), International Conference of Building Officials, Whittier, California.
Vasilopoulos, A. A. and Beskos, D. E. (2005), "seismic design of irregular space steel structures using advanced methods of analysis", Report No 7, Group of Analysis and Design of Steel Structures, Department of Civil Engineering, University of Patras, Patras, Greece, November.
Vasilopoulos, A. A. and Beskos, D. E. (2006 & 2007), "Seismic design of plane steel frames using advanced methods of analysis", *Soil Dyn. Earthq. Eng.*, 2006; **26**: 1077-1100 & Corrigendum, 2007; **27**: 189.
Vasilopoulos, A. A. and Beskos. D. E. (2008), "Seismic design of space steel frames using advanced methods of analysis", *Soil Dyn. Earthq. Eng.*, in press.

DN